Finite Element Structural Analysis Evaluating New Retrieval Strategies in the Hanford Waste Tanks [1] - 19125

Ken I. Johnson*, Naveen K. Karri*, John E. Deibler*,
F. George Abatt**, Ken L. Stoops**, Larry J. Julyk**, Brian M. Larsen**,
*Pacific Northwest National Laboratory, Richland, Washington 99352
** Becht Engineering Co., Inc., Richland, Washington 99352

ABSTRACT

Several waste retrieval methods being considered for the Hanford underground single- and double-shell nuclear waste storage tanks would require changes to the equipment loads above the tanks or structural modifications to the tanks themselves. Detailed structural analysis has been used in the planning phase to ensure that the reinforced concrete tanks continue to meet structural design codes in the modified configuration of these waste retrieval options. The feasibility of installing new single and multiple large risers penetrating the tank dome was evaluated using this approach. This paper summarizes the structural analysis methods and design codes used to evaluate the introduction of new unreinforced penetrations in a single-shell tank dome. The anticipated equipment loads during current and future waste retrieval operations are evaluated to ensure the continued structural integrity of the tank under thermal, dead weight, and seismic loads.

INTRODUCTION

The feasibility of applying proposed waste retrieval methods in the Hanford single- and double-shell waste tanks is thoroughly reviewed before they are considered for implementation. That review includes detailed structural analysis for retrieval options that require modifying the tank structure or the loads applied to the tanks. The option to install new risers in the tank domes has been considered because of the potential to reduce the overall time and cost required to retrieve the waste and prepare the tanks for closure. This paper describes the structural analyses performed to confirm the continued structural integrity of a single-shell tank (SST) with new dome penetrations and retrieval equipment loads on the soil above the tank dome. The paper describes the detailed finite element models used to analyze the tank response to the static thermal and operating loads plus the dynamic seismic loads. The paper then summarizes the systematic methods used to reduce the finite element results to global concrete section demands vs. capacities and local rebar and concrete stresses near the cut surface of the penetration. Example results are presented that confirm that penetrations could be cut in the tank domes and not unduly jeopardize the structural integrity of the tank.

Prior to studying the proposed dome penetrations, a structural Analysis of Record (AOR) was completed in 2015 of the four SST designs at the Hanford Site [1]. There are 149 SSTs (with 208, 2006, 2869, and 3785 m^3 storage capacities) located in twelve SST-Farms that were constructed between 1943 and 1964. Finite element models were used to predict the structural response of the SSTs to the historical thermal and operating loads, plus current site-specific design basis seismic loads. The combined responses of the concrete tank to the static and seismic loads were then evaluated against the design requirements of the

[1] This manuscript has been authored by Battelle Memorial Institute, Pacific Northwest Division, under Contract No. DE-AC06-76RL0 1830 with the U.S. Department of Energy. The publisher, by accepting the article for publication, acknowledges that the United States Government retains a non-exclusive, paid-up, irrevocable, world-wide license to publish or reproduce the published form of this manuscript, or allow others to do so, for United States Government purposes.

American Concrete Institute code, ACI-349-06, for nuclear safety-related concrete structures [2]. The AOR determined that, including the bounding effects of their operating histories, each of the four major tank designs currently satisfies the ACI-349-06 structural design requirements. The static and seismic finite element models developed and verified in the AOR provided the basis for the current analysis of post-construction penetrations in a SST dome.

THERMAL AND OPERATING LOADS ANALYSIS

The thermal and operating loads analysis (TOLA) modified the Type-IV AOR thermal-structural model described in [3] to include penetrations in the dome. The Type-IV SSTs are 22.9 meters (75 feet) in diameter and approximately 13.4 meters (44 feet) from floor to dome center. While the Type-IV SSTs had a 3785 m^3 storage capacity during use, all free liquids have now been removed from the solid waste that remains in the SSTs. The remaining waste in the tanks studied is in the form of sludge or saltcake to a depth of about 1.3 m (50 inches). Fig. 1(a) shows the half symmetry (180°) finite element mesh with one post-construction dome penetration and the locations around the tank cross-section where the structural integrity evaluation is conducted. Fig. 1(b) is a conceptual sketch of the penetration and the riser completion. The riser will be installed through the penetration and supported by the concrete pad at grade.

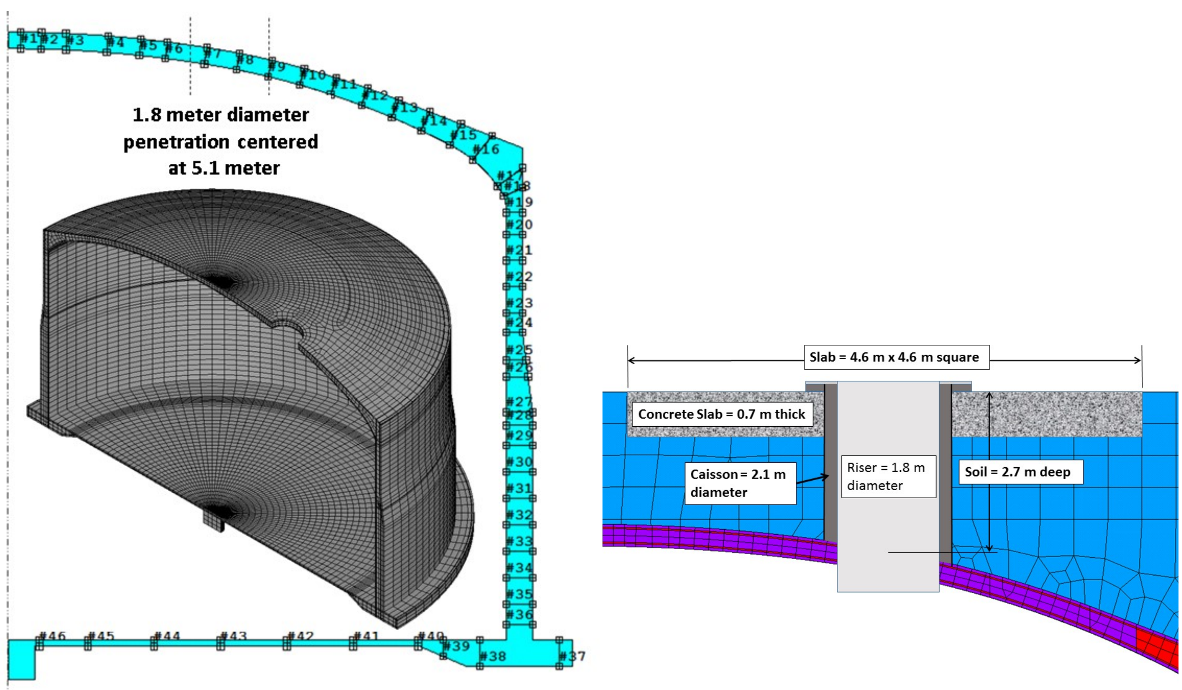

(a) **(b)**

Fig. 1. (a) Tank Mesh and ACI Evaluation Sections (b) Penetration Design Concept

The TOLA and seismic analyses are conducted separately because they simulate different characteristics of the tank response to static (deadweight and thermal) and dynamic (seismic) loads. As such, there are different finite element methods required in the static versus the soil-structure-interaction (SSI) seismic models. The TOLA model evaluates the degraded condition of the reinforced concrete tanks by including temperature dependent concrete stiffness, strength, and cracking. The model also includes elastic rebar, pressure dependent Drucker-Prager soil yielding, and contact between the soil and the concrete tank. In comparison, the seismic analysis uses a transient-dynamic model with elastic soil and concrete properties, and contact between the soil and concrete. Both the TOLA and seismic models incorporate one or more vertical slip rings in the soil above the dome to ensure that soil bridging does not artificially reduce the soil loads on the tank dome. The models also adjust the sidewall contact interferences to enforce the at-rest soil pressures (50% of the soil weight at depth) that are expected from the construction soil layering and compaction refill process used during construction.

The seismic model also requires the inclusion of layered linear dynamic soil properties, dynamic friction coefficients between soil and concrete tank interfaces, and the soil model must be extended below the tank and radially at a greater distance than is needed in the static model. Uncertainty in soil properties is addressed through multiple seismic analyses with lower-bound, best-estimate, and upper-bound dynamic soil properties. In addition, to achieve the seismic solutions in a reasonable time with given computer resources, the concrete is modeled with linear shell elements with the degraded orthotropic properties obtained from the TOLA analysis. Hence, there is no modeling of potential subsequent concrete cracking or cyclic softening in the SSI seismic analysis. To compensate, fully cracked section properties are used and it is noted that the seismic induced cyclic stress resultants are typically small compared to the static resultants thus limiting any potential cyclic softening.

Bounding thermal histories were established from waste temperature records [Fig. 2(a)] and applied to the model [Fig. 2(b)] to include the thermal degradation of concrete modulus and strength, plus cracking due to differential thermal expansion under in situ deadweight loads. As shown in Fig. 2(a), different profiles were developed for the tank floor, wall, and dome sections based on the available tank waste and wall temperature data discussed in detail in the Type-IV AOR report [3]. The current analysis employs a simplified version of these profiles, which was also discussed in that report. The degraded stiffness of the concrete exposed to high operating temperatures is also incorporated in the seismic analysis by degrading the stiffness properties of the shell elements used to simulate the tank.

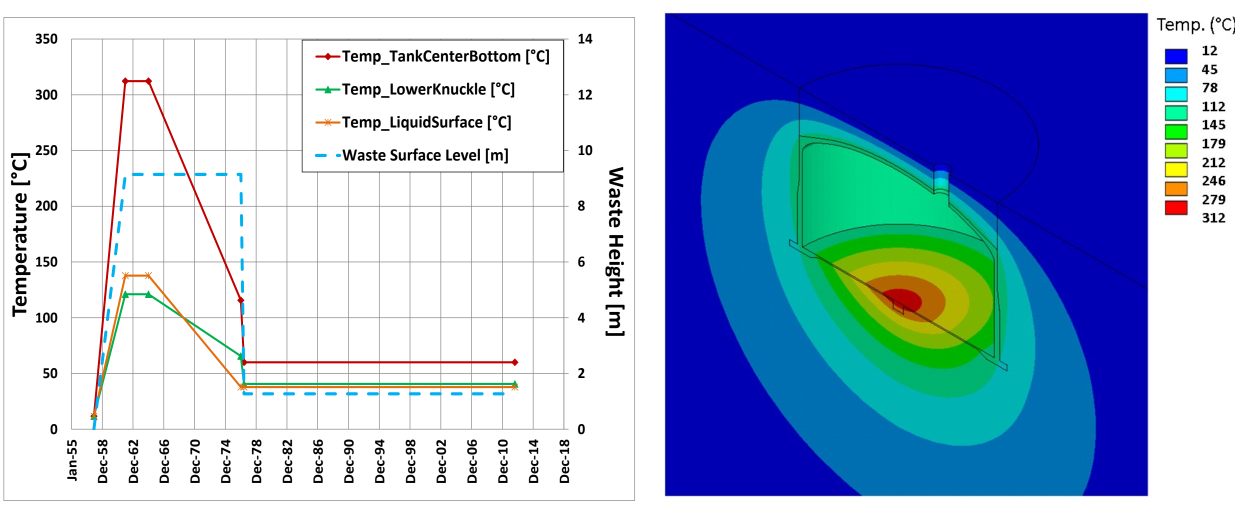

(a) (b)

Fig. 2. (a) Thermal History and (b) Peak Temperature Profile in the TOLA Model

DYNAMIC SEISMIC ANALYSIS

The seismic model is based on the existing AOR model, which was reviewed and approved during the Type-IV AOR [3]. The AOR model was modified to include the proposed large penetrations in the tank dome.

The soil-structure interaction seismic models were created and analyzed in the time domain using version 13.0 of the general-purpose finite element program, ANSYS® [2] [4]. The Evaluation Criteria [5] defined the maximum considered earthquake (MCE) ground motions as the ground motions with a mean annual exceedance frequency of 1 in 2500 years (2% probability of exceedance in 50 years). In this analysis, the site-specific design response spectra for the SST facilities uses the design spectra of the Hanford Tank Waste Treatment and Immobilization Plant (located in the 200 East Area) as a reasonable assessment of the current state of knowledge of the seismic hazard levels at the Hanford 200 East and 200 West areas where the SSTs are located. Because the SSTs are designated as Performance Category 2 (PC-2) structures, the SST ground motions are developed as 2/3 of the Hanford Site MCE ground motion.

A half-symmetry (180°) model of the SST, including the concrete tank and surrounding soil, was developed to evaluate the SSI response of the tank with either one or four penetrations in the dome (see Fig. 3). The tank concrete was modeled with ANSYS® SHELL181 (4-node finite strain shell) elements at the mid-line profile of the tank cross-section. The soil is modeled with ANSYS® SOLID45 linear elastic volumetric elements. The seismic model includes both backfill soil properties and far-field soil properties. The concrete properties assigned to the models are degraded properties developed from the TOLA analysis.

To facilitate detailed evaluation of local demands near the penetration, the tank dome has a refined mesh near the penetration extending radially outward for 0.9 meter (3 feet), which then transitions out to the global mesh. The modifications to the soil mesh are similar. Spar elements were added to support the hole and act as a caisson holding back the soil surrounding the penetration.

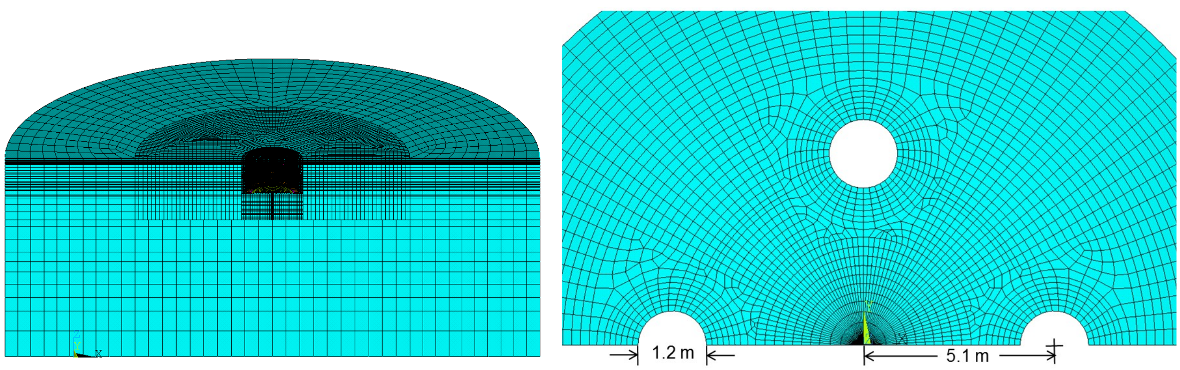

Fig. 3. Global Seismic ANSYS Model and Concrete Dome Mesh Detail

The seismic model includes contact interfaces between the tank and the surrounding soil, between the tank waste and the inner surface of the tank wall, and within the soil above the tank dome. The contacts are allowed to slide and separate at the interface between the tank and the soil, and are allowed to slide but not separate within the soil. The contact interfaces constitute the only nonlinearities in the seismic model.

Contacts are used in the soil above the tank dome to prevent or minimize soil arching. In the seismic models, vertical contact surfaces are inserted into the overburden to create annular rings of soil that are free to displace vertically with the tank roof, but allow the load to transfer laterally during horizontal motion. This effectively creates a nonlinear yield mechanism that acts in the vertical direction only. The

[2] ANSYS is a registered trademark of ANSYS, Inc., Canonsburg, PA

effectiveness of this technique was demonstrated by matching the theoretical at-rest soil pressure on the dome.

Additional mass is added to the soil surface above the dome center and penetrations to simulate concentrated loads such as tank pits and permanent or temporary equipment. The magnitude of the mass is applied in accordance with the Hanford tank dome load controls and the mass of retrieval equipment at the penetration.

A lateral boundary distance of at least 97.5 m (320 feet) was chosen for the cylindrical mesh based on spectral matching of the model boundary spectra with the free-field spectra at the corresponding elevation. All nodes on the periphery of the model were "slaved" to a single node at each layer to force the soil to behave essentially as a shear beam.

The soil depth is selected in accordance with ASCE [6] such that the shear wave velocity at the base is greater than or equal to 1,067 m/s (3,500 ft/s), or else the base is at least three times the maximum foundation dimension below the foundation.

The free-field seismic model input motion developed for the AOR of each tank type using SHAKE [7] was calibrated for use in ANSYS® through spectral matching to ensure that the ANSYS® SSI model reproduced or bounded the corresponding free-field response at the tank foundation elevation and at the soil surface. Calibration was necessary because SHAKE operates in the frequency domain and ANSYS® operates in the time domain. Thus, factors such as damping and boundary conditions operate differently between the two programs. Spectral matching criteria were used to ensure that the spectra corresponding to the ANSYS® input seismic acceleration time series appropriately matched the SHAKE target spectra. This resulted in a conservative margin between the ANSYS® seismic response spectra and the corresponding SHAKE target spectra. The margin is particularly significant for frequencies above 2.5 Hz for the horizontal ground motion and above 8 Hz for the vertical ground motion. Therefore, the reported seismic demands are likely to be conservative by 20% to 40% as shown in the upper curve of Fig. 4.

A large point mass element (more than 100 times the mass of the full model) is located at the base of the model and the seismic excitation is applied at that node as a transient force corresponding to the known acceleration at the base of the model. All nodes at the base elevation of the model are coupled to the point mass to create a rigid region. Because the ANSYS SSI model has a rigid base that will reflect downward propagating waves, the prescribed input motions are the in-column motions generated by the program SHAKE. The in-column motions are appropriate because they represent the superposition of both the upward and downward propagating waves at the location of the rigid boundary.

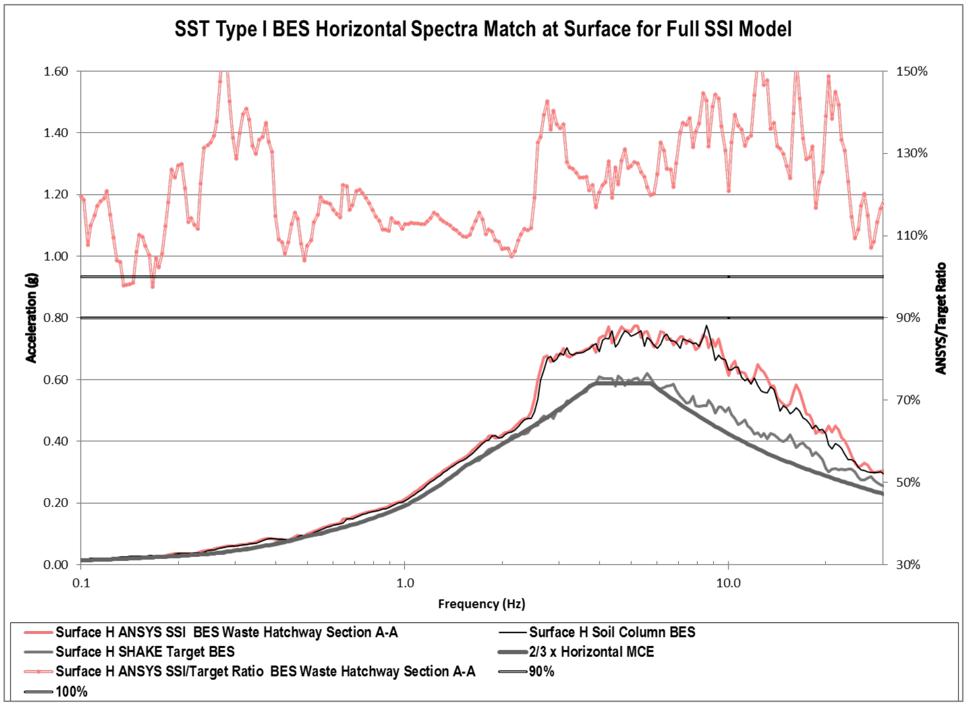

Fig. 4. Comparison of Best Estimate Soil (BES) Horizontal Surface Spectra from the ANSYS® and SHAKE SSI Models (Typical for all SST types)

Two-directional seismic excitation is applied as horizontal excitation parallel to the symmetry plane and vertical excitation. The horizontal excitation consists of vertically propagating (horizontal) shear waves and the vertical excitation consists of vertically propagating compression waves. Both directions of input are applied simultaneously. Loading is applied to the model in two steps: initial gravity and seismic excitation. The initial gravity step establishes the proper geostatic conditions for the subsequent seismic loading. The resulting deadweight plus seismic forces and moments obtained from the SSI analysis are extracted from the tank degraded concrete shell elements and post-processed to produce seismic-only resultant tank section loads throughout the tank structure for evaluation in combination with the TOLA results. The post-processing uses an enveloping process to produce bounding seismic resultant loads that are conservative in space (circumferentially) and time.

In addition to the global post processing, local post-processing is performed near the penetration to support working stress evaluations in combination with the TOLA results. The local post-processing method is the same as the global method, except that the orientation of the local results is transformed from the global cylindrical orientation to a local cylindrical orientation about the penetration center.

STRUCTURAL EVALUATION METHODS

When rebars are cut to make a dome penetration, the strength of the reinforced concrete dome sections close to the penetration are reduced. The cut rebars do not develop their full strength until a distance known as the rebar "development length" away from the hole. Therefore, the local rebar and concrete stresses near the hole must be evaluated as well as the global sections away from the penetration.

The global section evaluations are performed using the ultimate strength method in Section 9.2 of the ACI-349-06 code [2]. ACI-349-06 load combinations 1, 4, and 9 are appropriate for the SST structural integrity evaluations. These factored load combinations are defined as follows:

Load Combination 1 (LC1). $U = 1.4D + 1.4F + 1.7L + 1.7H$ (Eq. 1)

Load Combination 4 (LC4). $U = D + F + L + H + T_o + E_{ss}$ (Eq. 2)

Load Combination 9 (LC9). $U = 1.05D + 1.05F + 1.3L + 1.3H + 1.05T_o$ (Eq. 3)

The section demands (U) are defined as factored combinations of dead loads (D), live loads (L), fluid pressure loads (F), loads due to adjacent soil pressure (H), thermal loads (T_o), and seismic loads (E_{ss}). The scale factors are applied to the individual load types (rather than to the model results) so that nonlinear concrete cracking is correctly included for factored loads.

This paper presents the LC4 combination of static TOLA plus seismic loads as an example of the evaluation methods used in the structural integrity assessment of the Hanford waste tanks. The analyses consider the previous load histories of the tanks plus potential new loads associated with waste retrieval operations as well as the local seismic hazard. The LC4 evaluation is particularly important because the seismic induced vibrational response of the tanks has the potential to cause tensile cracking or local exceedance of the section capacity where the net compressive response of the tank under factored static loads (LC1) may not. Note also that the previous SST Type IV AOR in [3] showed that the LC9 combinations had significantly lower demand vs. capacity ratios compared to the LC1 and LC4 load cases. Therefore, the LC4 evaluation is presented in this current demonstration.

The Hanford tanks include existing dome penetrations that were designed with additional rebar to resist the load concentrating effect of the hole. Since post construction penetrations do not include this added reinforcement, it is important to locate them in an area of the arched dome where the reinforced concrete will remain in hoop and radial compression under the expected load combinations. The finite element section force and moment demands predict that the dome center remains in hoop and radial compression to a radius of 6.4 meters (21 feet) for the combined TOLA and seismic loads. Fig. 5 shows a 1.8 meter (6 foot) diameter penetration overlaid on the design rebar pattern of the tank. The penetration is centered at 5.1 meter (16.75 feet) from the dome center so that the outer cut surface at 6 meter (19.75 feet) is within the compression zone. The section forces and moments near the penetration were also evaluated to determine the area of influence of the penetration on the load distributions in the dome. The forces and moments reduce to the undisturbed values at a distance of about 2.2 penetration diameters from the penetration center. Therefore, the minimum center-to-center distance of 4.5 diameters between multiple penetrations was imposed to ensure that adjacent penetrations do not interact structurally.

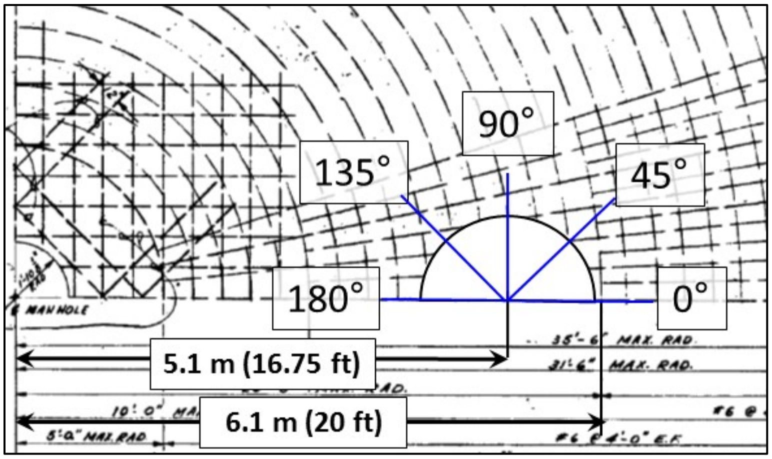

Fig. 5. The 1.8 meter (6 foot) diameter penetration located in the design rebar pattern. Angles are shown where the local rebar and concrete stresses are evaluated.

In addition to the thermal history the load combination addressed in this paper is shown in Fig. 6. The dome loads are concentrated in 6.1 meter (20 foot) diameter circles above the dome center or above the 1.8 meter (6 foot) diameter penetration. The 136 metric ton (MT) (300 kip) concentrated load above the dome center conservatively accounts for the weight of existing equipment and the staging of retrieval equipment distributed on the soil above the tank dome. The 25 MT (55 kip) load above the penetration represents the net weight of the installed penetration illustrated in Fig. 1(b) before the installation of retrieval equipment.

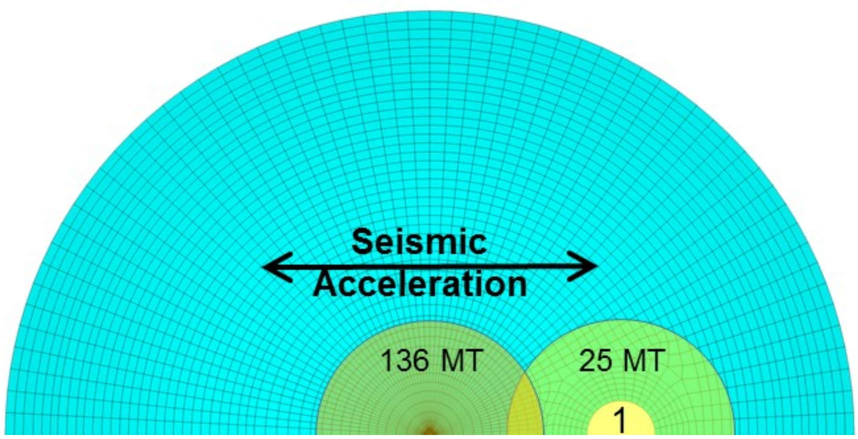

Fig. 6. Baseline Dome Load Profile with One Penetration

While this paper presents a single example of the analyses considered, a variety of loading conditions were evaluated as well as additional configurations with four penetrations as shown in Fig. 7. The 93 MT (205 kip) concentrated loads in Figure 7 represent the 25 MT (55 kip) net weight of the installed penetration plus a conservative 68 MT (150 kip) estimate of retrieval equipment loads.

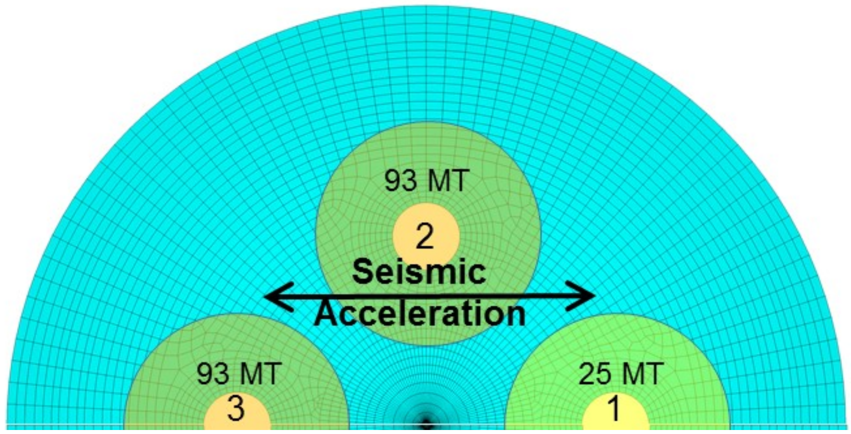

Fig. 7. Example One-Half Symmetry Model of Four Penetrations (results not reported here)

The LC4 Demand-Capacity Evaluation of Global Tank Sections

When performing structural integrity analysis of the Hanford tanks, it is important to distinguish between 1) structural response predictions for the prescribed load combinations and 2) structural adequacy evaluations. In general, structural response predictions are based on best-estimate or mean mechanical properties. Then, having obtained the best-estimate demands (the section force, moment, and shear loads), the structural adequacy should be evaluated based on the minimum specified strengths. As such, the static and seismic finite element models described in this paper use the best estimate strength and stiffness properties of the concrete tank for the bounding thermal history for the Type IV SSTs, and perform the ACI-349 integrity evaluation using the 95/95 lower bound concrete strength at the maximum local concrete temperatures predicted by the thermal analysis of the tank operating history. Therefore, best-estimate concrete stiffness is used to calculate the best estimate of force and moment loads on the tank whereas the lower-bound concrete strength at maximum temperature is used to conservatively determine the structural margins.

The ACI-349 demand-capacity evaluation is conducted for the global tank sections that are more than the rebar development length away from the penetration. The section capacities calculated according to ACI-349, Section 10, include the interaction of axial force and moment [2]. Fig. 8 shows a typical force-moment interaction diagram for a reinforced concrete section in the tank dome. The enclosed curves define the +/- force-moment capacities from ACI-349, Section 10, for the rebar placement in the dome thickness and the 95/95 lower bound concrete strength at temperature. Fig. 8 shows two applied force-moment pairs (in the meridional and circumferential directions) where the demand is less than the capacity. The demand/capacity ratio can be defined as the ratio of the vector length from the origin to the force-moment demand coordinate divided by the vector length from the origin to the capacity curve with the same force to moment ratio. A demand/capacity ratio less than 1.0 indicates that the ACI requirements are met. Caution should be observed to not interpret the demand/capacity ratio as a measure of safety factor, which would only apply if the same force to moment ratio is maintained under increasing or decreasing loads.

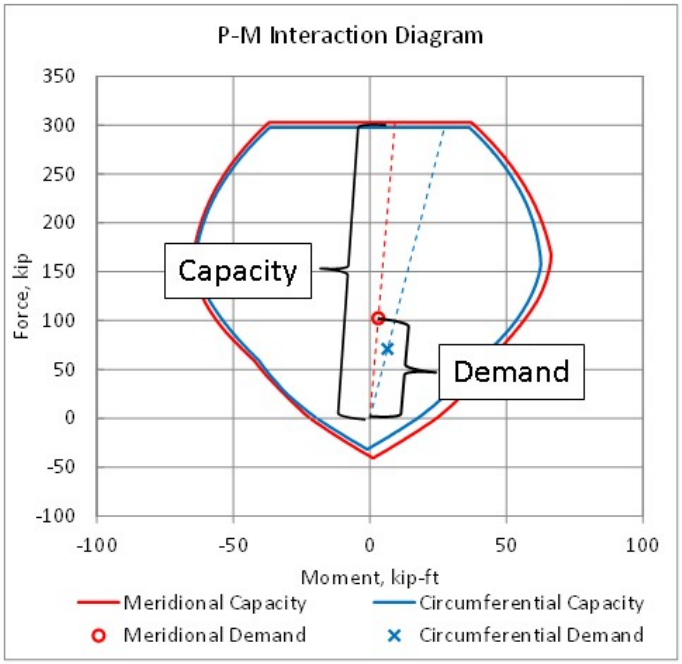

Fig. 8. Tank Dome Force-Moment Interaction Diagram

The global evaluation is conducted at the 46 tank sections from the dome center to the slab center shown in Fig. 1(a). The off-center penetration and loads require that the evaluation be performed at multiple angles around the 180° model to identify the maximum values. The LC4 TOLA plus seismic D/C ratios from the dome to slab center and angles 0° through 180° are plotted in Fig. 9 for the (a) meridional, (b) hoop, (c) through-wall shear, and (d) in-plane shear loads. The first peak in D/C ratio in the meridional direction is 0.6 at section 18 in Fig. 1(a) at the haunch transition between the dome and the wall. The second peak in meridional D/C is 0.5 at section 39 where the footing transitions to the slab. The highest peak in meridional D/C is 0.9 in the center of the slab. The peak at the center of the slab is due to the high historical waste temperature, and it is not significant because the slab is fully supported by the soil. The maximum D/C ratio in the hoop direction is 0.53 at section 12 in the dome. The maximum through-wall shear D/C ratio is 0.93 at section 19 where the haunch transitions to the top of the wall. The secondary peak in through-wall shear is at sections 38 through 40 where the footing transitions to the slab. Finally, the in-plane shear D/C ratio is a maximum of 0.5 at sections 7 through 9 near the penetration at 0°, but elsewhere it is less than 0.4 at section 24 in the wall. The results in Figure 9 illustrate that all of the global D/C ratios are less than 1.0 and the penetration at 0° does not significantly increase the loads outside of the immediate area. Therefore, the ACI-349 structural integrity requirements are shown to be met for this SST with the penetration and loads shown in Fig. 6. The analysis of four penetrations with the loads in Figure 7 also showed that the ACI-349 structural integrity requirements are met.

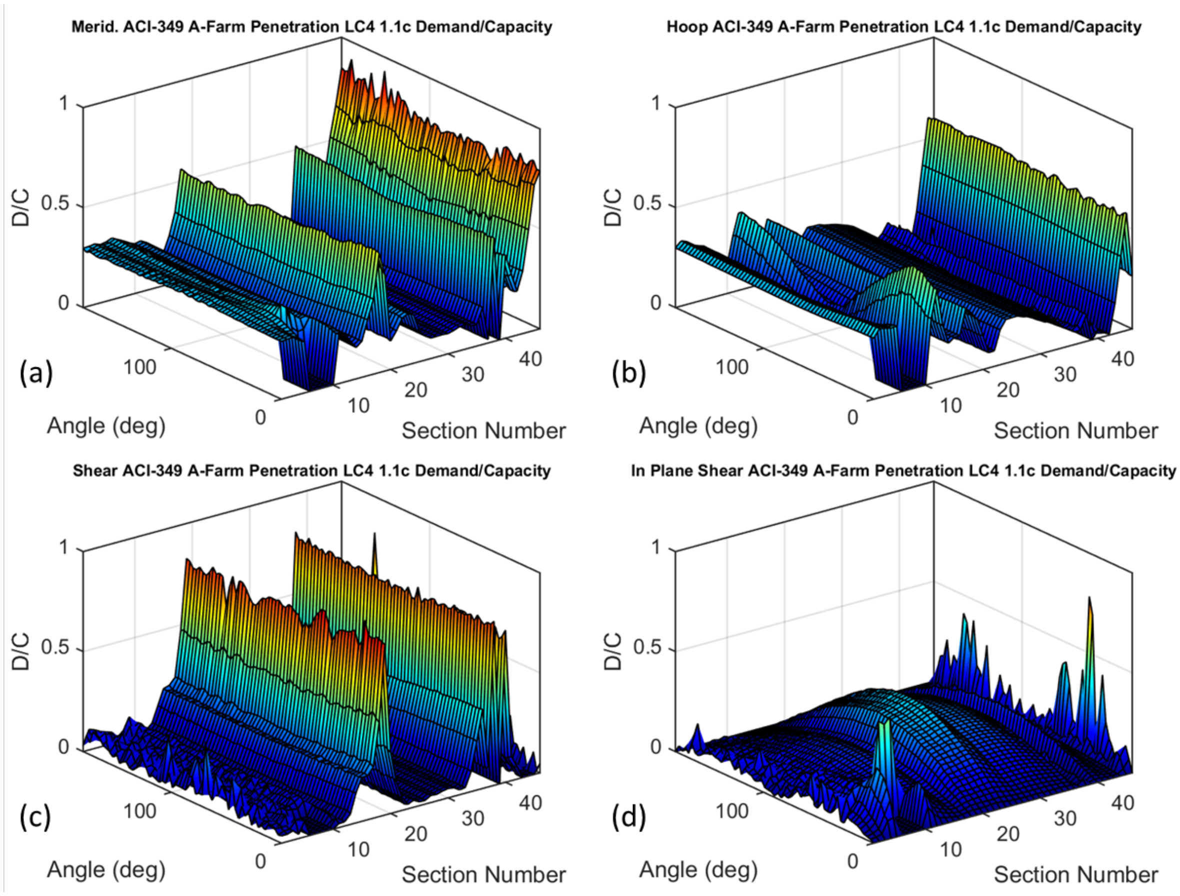

Fig. 9. Demand/Capacity Plots under ACI LC4 TOLA + Seismic Combinations (a) Meridional (b) Circumferential (c) Through-Wall Shear (d) In-Plane Shear

Local LC4 Evaluation of Rebar and Concrete Stresses Near the Penetrations

The section stresses near the cut surface of the hole must also be checked to ensure that rebar tension remains well below the rebar strength that develops at increasing distance into the concrete from the cut surface. The working stress method was used to evaluate the rebar and concrete stresses at the 0°, 90°, and 180° directions in Fig. 5 where the meridional and hoop rebars are normal and parallel to the cut surface. However, the concrete sections at the diagonal 45° and 135° orientations are evaluated as plain concrete because reinforcing bars are not oriented in the local hoop and radial directions there.

The working stress method calculates the rebar tensile and concrete compressive stresses assuming a linear strain distribution through distance "d" from the compressive face to the tensile rebar in the reinforced concrete section illustrated in Fig. 10(a). The method conservatively assumes that the rebar acts only in tension and the concrete only in compression. The rebar tension and maximum concrete compression are calculated using an iterative solution that adjusts the location of the neutral axis until the calculated moment equals the applied moment for the applied net section force.

The rebar development length was calculated to be 33 cm (13 inches) using the equation in ACI-318 Section 12.2.3 [8] for the specified placement of the #6 [19mm (0.75 inch) diameter] grade 40 rebars in the dome thickness. The rebar strength at shorter lengths can be conservatively estimated as the rebar yield strength, 276 MPa (40 ksi), times the ratio of the distance to the surface divided by the development length. With the short 33 cm (13 inch) development length, a rebar strength of 54.5 MPa (7.9 ksi) is already developed at 7.6 cm (3 inch) radial distance from the penetration cut surface.

The plain concrete design method in ACI-318 Section 22.5 credits concrete with supporting a limited tensile stress when the section is loaded in compression plus bending [8]. The method calculates the outer-fiber tensile and compressive stresses assuming elastic behavior of the full dome thickness. The bending stress resisting the section moment is added and subtracted from the net compressive stress to calculate the tensile and compressive stresses at the outermost fibers of the concrete section [see Figure 10(b)]. The maximum concrete tensile stress allowed by ACI-318 Section 22.5.3, Eqn 22-6 [8] is 1.13 MPa (164 psi) for the specified 20.7 MPa (3 ksi) 28-day design compressive strength of the concrete. Note that test results of concrete cores obtained from a SST dome (after installation of a center penetration) indicated significant higher concrete compressive strengths [9]. The average compressive strength of all the tested cores was about 55 MPa (8 ksi); more than 2.5 times the original 28-day specified design strength [9].

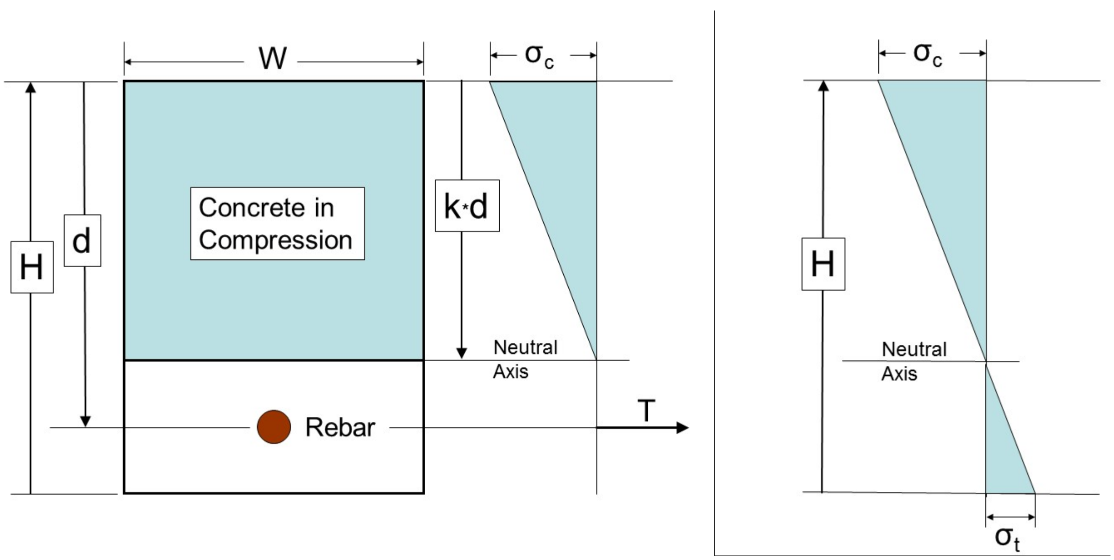

(a) **(b)**

Fig. 10. (a) Working Stresses in Rebar and Concrete, (b) Plain Concrete Stresses

The results in Fig. 11 show the rebar tension and concrete compression are low at distances of 7.6 to 91.4 cm (3 to 36 inches) from the cut surface of the penetration. Fig. 11(a) shows that rebar tension is very low compared to the 54.5 MPa (7.9 ksi) strength developed at 7.6 cm (3 inch) radial distance from the penetration cut surface. Note that the meridional rebar are in compression at 90° and the hoop rebar are also in compression at the 0°, 90°, and 180° directions. The maximum concrete compressive stress of 4.6 MPa (670 psi) in Fig. 11(b) is also low compared to the specified 20.7 MPa (3 ksi) 28-day design strength. The plain concrete evaluation of the 45° and 135° diagonals in Fig. 11(c) also shows that the maximum concrete tension is less than the ACI-318 tensile stress limit of 1.13 MPa (164 psi). The 3.26 MPa (473 psi) maximum compressive stress in Fig. 11(c) is also low compared to the 20.7 MPa (3 ksi) 28-day design strength. This analysis demonstrates that the rebar and concrete stresses around the new penetration would be acceptable under the combined TOLA and seismic loads.

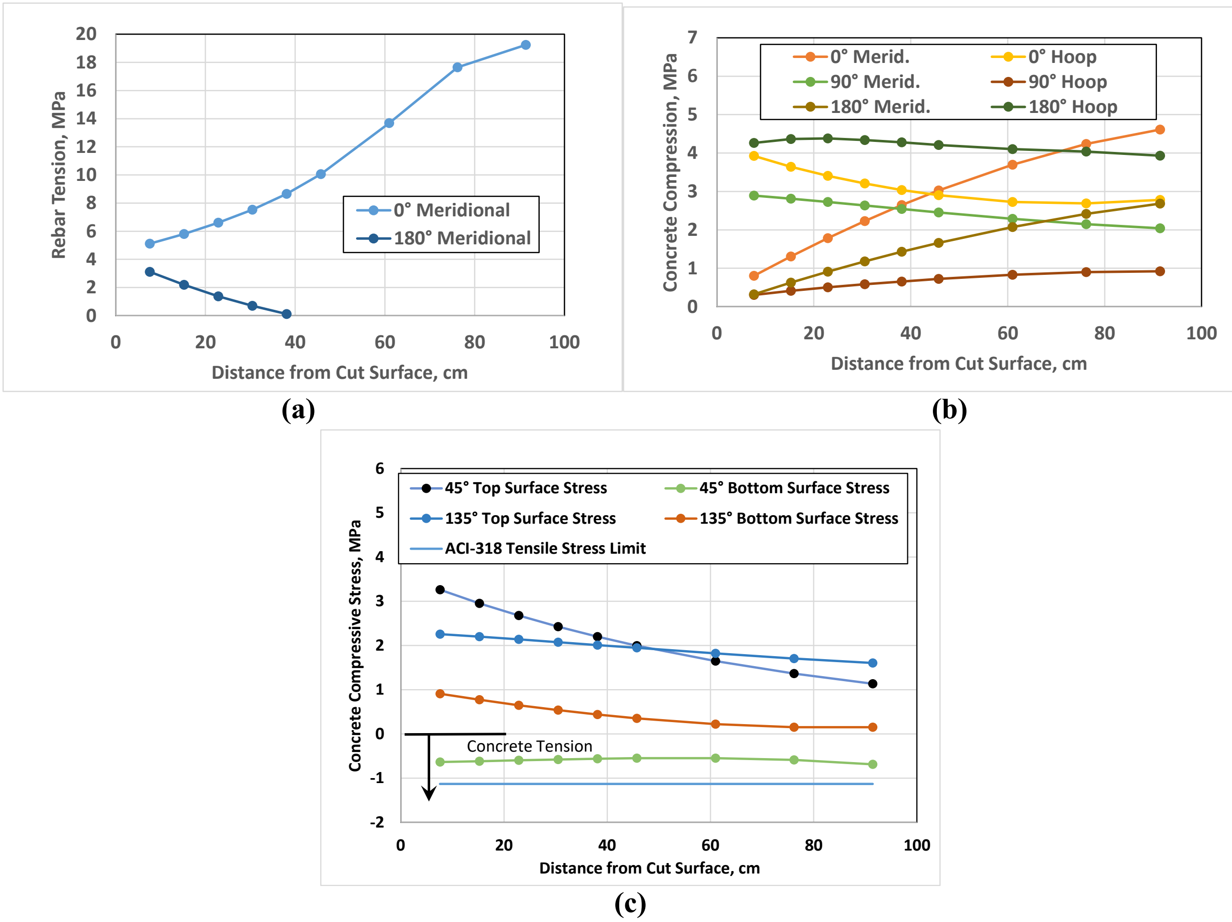

Fig. 11. (a) Rebar Tension at 0° and 180°, (b) Concrete Compression at 0°, 90°, 180°, and (c) Plain Concrete Stresses at the 45° and 135° Diagonals

CONCLUSIONS

This paper describes the detailed engineering methods used to assess how post-construction penetrations in the dome of a single-shell nuclear waste storage tank could affect the structural integrity of the Hanford waste tanks. The analyses identified the region of the arched tank dome where penetrations could be cut and the section force and moment demands would still be acceptable compared to the code-based structural capacities. Both the global section demands between penetrations and the local rebar and concrete stresses near the surface of the hole were found to be acceptably low for the loads evaluated. Therefore, conditions do exist where it would be structurally acceptable to install new penetrations in a SST dome to increase access to the tank interior. Increased access into the Hanford waste tanks has the potential to reduce the overall time and cost required to retrieve the waste and prepare the tanks for final closure.

ACKNOWLEDGEMENTS

The authors would like to acknowledge the Management and Engineering support of Washington River Protection Solutions and the funding provided on behalf of the U.S. Department of Energy, Office of River Protection to perform the structural analysis. The authors would also like to thank Dr. Robert P. Kennedy for his guidance and critical review of our engineering analysis methods.

REFERENCES

1. K. I. JOHNSON, J. E. DEIBLER, and N. K. KARRI. *Single-Shell Tank Integrity Project Analysis of Record: Summary Report for the Hanford Single-Shell Tank Structural Analyses of Record.* RPP-RPT-49994, Rev. 0. PNNL-24280. Pacific Northwest National Laboratory, Richland, Washington (2015).

2. ACI. *American Concrete Institute Code Requirements for Nuclear Safety Related Concrete Structures*. ACI 349-06, American Concrete Institute, Farmington Hills, Michigan (2007).

3. K. I. JOHNSON, S. P. BAPANAPALLI, J. E. DEIBLER, F. G. ABATT, K. L. STOOPS, N. K KARRI, S. E. SANBORN, S. P. PILLI, B. M. LARSEN and L. J. JULYK. *Single-Shell Tank Integrity Project Analysis of Record: Hanford Type IV Single-Shell Tank Thermal and Operating Loads and Seismic Analysis*. RPP-RPT-49992, Rev. 0; PNNL-23341, Rev. 0, Pacific Northwest National Laboratory, Richland, Washington (2014).

4. ANSYS. *User's Manual Version 13.0*, ANSYS, Inc., Canonsburg, PA (2010).

5. K. I. JOHNSON, J. E. DEIBLER, F. G. ABATT, and M. W. RINKER. 2010. *Single-Shell Tank Structural Evaluation Criteria.* RPP-46442, Rev. 0, Pacific Northwest National Laboratory, Richland, Washington (2010).

6. ASCE. *Seismic Analysis of Safety-Related Nuclear Structures and Commentary*, ASCE 4-98. American Society of Civil Engineers, Reston, Virginia (2000).

7. P. B. SCHNABEL, J. LYSMER, and H. B. SEED. *SHAKE – A Computer Program for Earthquake Response Analysis of Horizontally Layered Sites*. Earthquake Research Center, University of California, Berkeley, California, EERC 72-12 (1972).

8. ACI. *Building Code Requirements for Structural Concrete (ACI 318-05) and Commentary (ACI 318R-05)*. American Concrete Institute, Farmington Hills, Michigan. ISBN 978-0870311710 (2005).

9. R.S. RAST. *Inspection and Test Report for the Removed 241-C-107 Dome Concrete*. RPP-RPT-50934, Rev. 0, Washington River Protection Solutions, Richland, Washington (2013).